Journal of Molecular Liquids 332 (2021) 115842

Contents lists available at ScienceDirect

Journal of Molecular Liquids

journal homepage: www.elsevier.com/locate/molliq

Effect of the surfactant head-group size dependence of the dye-surfactant interactions on the lyotropic uniaxial to biaxial nematic phase transitions

Erol Akpinar [a,*], Nazli Uygur [a], Oznur Demir Ordu [a], Dennys Reis [b], Antônio Martins Figueiredo Neto [b]

[a] Bolu Abant Izzet Baysal University, Faculty of Arts and Sciences, Department of Chemistry, 14030 Golkoy, Bolu, Turkey
[b] Universidade de Sao Paulo, Instituto de Fisica, Rua do Matao, No. 1371, 05508-090, Sao Paulo, SP, Brazil

ARTICLE INFO

Article history:
Received 8 January 2021
Received in revised form 19 February 2021
Accepted 1 March 2021
Available online 4 March 2021

Keywords:
Lyotropic uniaxial and biaxial nematic phases
Anionic azo dye Sunset Yellow
Surfactant-dye interaction
Polarizing optical microscopy
Laser conoscopy
Small-angle X-ray scattering

ABSTRACT

In the present study, the interactions of the anionic azo dye Sunset Yellow with dodecylalkylammonium bromide (DAABr) surfactants in lyotropic mixtures have been investigated for the stabilization of the different lyotropic nematic phases. Sunset Yellow doped mixtures of DAABr surfactants, with different head-group size, were studied by polarizing optical microscopy, laser conoscopy, and small-angle X-ray scattering. It was found that the extent of the interaction of Sunset Yellow with DAABr surfactant head groups on micelle surfaces affects the stabilization of different nematic phases, by causing the change in the micellar structural parameters. The results also indicated that the micelle surface curvature should be different in the three nematic phases.

1. Introduction

Understanding the stabilization of the lyotropic uniaxial and biaxial nematic phases is an active experimental research field. Mainly, the important feature of uniaxial lyotropic nematic phases which attracts the attention of the researchers is the preferred alignment of their phase directors with respect to the applied magnetic field. This preferential alignment is also an important parameter in the classification of lyotropic nematic phases and arises from the diamagnetic susceptibility of the surfactant alkyl chains [1–3]. Three types of lyotropic nematic phases were identified. In the uniaxial discotic (N_D) and calamitic (N_C) nematic phases, the director $\vec{n}$ aligns perpendicular and parallel to the magnetic field direction, respectively, in the case of the main amphiphile having carbonic chains. There exist two optical axes and three orthogonal two-fold symmetry axes, $\vec{l}$, $\vec{m}$ and $\vec{n}$, where $\vec{n} = \vec{l} \times \vec{m}$ [4–8] in the lyotropic biaxial nematic phase (N_B). Furthermore, the experimental studies proved that, in general, the N_B phase region is located between the two uniaxial nematic phases in the phase diagrams [9–11]. Moreover, the transitions from the N_B phase to the N_D or N_C phases are of second order, as theoretically predicted [12,13].

In early studies, researchers focused on whether the N_B phase was a distinct thermodynamically stable phase [10,14–20]. Recent studies have contributed to clarify the stabilization mechanism of the different nematic phases and also to find the factors for obtaining the biaxial nematic phase [21–25]. These factors were revealed from the perspective of choosing the suitable constituents of lyotropic mixtures by examining inter- and intra-aggregates (i.e., micelles) interactions. The structural units of the lyotropic nematic phases, 'micelles' formed by surfactants, are very sensitive to modifications both in the micelle core and on the micelle surfaces. For instance, the relative alkyl-chain lengths of surfactants (n_{surf}) [25] and cosurfactants (n_{cosurf}) [21] play a key role on the stabilization of uniaxial and biaxial nematic phases. The biaxial nematic phase domain in a partial phase diagram can be observed if $n_{cosurf} = n_{surf} \pm 2$, at least for the chosen surfactant/cosurfactant systems in [21,25]. Because the alkyl chains of both surfactants and cosurfactants have non-polar character, the $n_{cosurf} = n_{surf} \pm 2$ rule is mainly related to the effect of the interactions between those alkyl chains in the micelle core.

The interactions on the micelle surfaces are also important, similarly to the interactions in the interior of the micelles. In the case of the micelles with ionic surfactants, there exist repulsions between the surfactant head groups on the micelle surfaces. Different types of nematic phases may be obtained by controlling the characteristics of these repulsions. For instance, when an electrolyte is added to the lyotropic mixture, its oppositely charged ions are bound to the surfactant head groups, decreasing the micelle surface curvature strongly or loosely [26], due to the screening of the repulsions [27–29]. In the former and latter cases, the stabilization of the N_D and N_C is more favored, respectively, and intermediate level of the interactions between ions and head groups is responsible for the stabilization of the N_B [11,24].

* Corresponding author.
E-mail address: akpinar_e@ibu.edu.tr (E. Akpinar).

https://doi.org/10.1016/j.molliq.2021.115842
0167-7322/

Surfactant-electrolyte ions interactions are also important in isotropic dilute-aqueous solutions [27,30–32], which may be assumed as the precursors of the lyotropic nematic phases [22,24]. Because both systems consist of the same structural units, i.e., 'micelles', information obtained from one system can be useful to the other [24,33]. For instance, the presence of the electrolyte ions causes the increase in micelle size [34,35], leading to the packing of larger amount of the surfactant molecules in the micelles, in the isotropic [7,36,37] and lyotropic [33,38,39] solutions of surfactants. The change in micelle shape anisotropy, especially for the lyotropic nematic phases, is related to the extent of interactions between ionic species, surfactant head groups and ions of the electrolytes present in the solution. Experimental studies indicated that the extent of those interactions is based on the "kosmotropic" and "chaotropic" character of the ionic species [11,22–24]. Collins et al. summarily defined these two characteristic properties of the ionic species as the more or less hydration of the ions by surrounding water molecules [40,41]. The ionic species with similar extent of the kosmotropic/chaotropic characters leads to the formation of close contact ion pairs [42–45].

In a previous study, we investigated the isotropic micellar solution and lyotropic nematic phase properties of some tetradecylalkylammonium bromides by changing their head-group sizes [11]. That study mainly focused on the effect of the interactions between the conventional inorganic salt (electrolyte) ions, considering the Hofmeister series anions, and surfactant head groups with different sizes. The results indicated that those interactions are very effective on the stabilization of different lyotropic nematic phases. The information obtained from the isotropic micellar aqueous solutions of tetradecylalkylammonium bromides/inorganic salts gave valuable hints for the interpretation of the interactions observed in the lyotropic nematic phases.

Another important type of interaction in micellar solutions is the surfactant-dye interactions, which are crucial for some industrial and biotechnological applications in the dilute isotropic micellar solutions [46–54]. Recently, the effect of the presence of the azo dye 'Sunset Yellow', which consists of polyaromatic planar core and ionic parts at the periphery, has been investigated in the lyotropic mixtures of dodecyltrimethylammonium bromide/Sunset Yellow/1-dodecanol/water. It was shown that Sunset Yellow can be bound to the micelle surface stronger than the conventional inorganic electrolyte ions and gives larger biaxial nematic phase domain in the phase diagrams [55]. Thus, dye molecules may be used to stabilize different lyotropic nematic phases instead of the inorganic salts to obtain larger temperature range of the biaxial nematic phase.

In 2013, Cheng et al. studied one-dimensional nano-structured aggregate properties of some anionic azo dyes, including Sunset Yellow, in terms of their interactions with cationic conventional and gemini surfactants [56]. In general, while those dyes, except Sunset Yellow, produced nano-structured aggregates (nano-fibers, nano-helixes or nano-rods) with gemini surfactants, Sunset Yellow gave block-type aggregate with the same gemini surfactant as a result of the decrease in the interaction between dyes and surfactants. In the same study, authors also investigated the interactions of the dyes, which formed the nano-structured aggregates, with dodecyltrimethylammonium bromide (DTMABr), dodecyltriethylammonium bromide (DTEABr) and dodecyltripropylammonium bromide (DTPABr). They concluded that, as the surfactant head-group size gets larger, the curvature of the aggregates increases. Similar to the case of dye-gemini surfactant mixed systems, the interaction between the dyes and the conventional surfactants is stronger in dyes/DTMABr and weaker in dyes/DTPABr mixed systems. Thus, it is clear that the interactions of dyes with surfactants depend on the size of the surfactant head group.

While the effect of the dye-surfactant interactions depending on the surfactant head groups was reported in the literature in isotropic micellar solutions, this effect has not been systematically studied in the nematic phases of lyotropic liquid crystals to obtain biaxial nematic phase. In the present study we examine the stabilization of different lyotropic nematic phases, especially the biaxial one, from the surfactant head-group size dependence of the dye-surfactant interactions point of view. For this purpose, some dodecylalkylammonium bromide surfactants with different head-group sizes were used to prepare mixtures presenting the lyotropic nematic phases. The effects of the interaction of Sunset Yellow with those surfactants were investigated via polarizing optical microscopy, laser conoscopy and small-angle X-ray scattering. The results indicated, as we will show in the further parts of the present study, that the degree of the interactions between the surfactant head groups and Sunset Yellow influences the stabilization of the different lyotropic nematic phases.

2. Experimental

2.1. Materials

Dodecyltrimethylammonium bromide (DTMABr), dodecyldimethylethylammonium bromide (DDMEABr), 1-bromododecane, alkylamines (dodecylamine, *N*-methyldodecylamine, *N*,*N*-dimethyldodecylamine, diethylmethylamine and triethylamine), hydrobromic acid (HBr_{aq}) and 1-dodecanol (DDeOH) were purchased from Sigma-Aldrich and Merck with a purity of >98–99%. The anionic azo dye, Sunset Yellow (SSY), was also commercially available from Sigma-Aldrich with a dye content of 90% and it was purified three times considering the procedure given in [57,58]. The purification degree of the Sunset Yellow was confirmed from the phase transition temperatures of 30% aqueous lyotropic chromonic solution of Sunset Yellow, as described in [55]. Ultrapure water, provided by the Millipore Direct-Q3 UV purification system with 18.2 MΩ.cm of resistivity at 25 °C, was used for the preparation of lyotropic liquid crystalline mixtures.

2.2. Synthesis and characterization of surfactants

DTMABr and DDMEABr are commercially available surfactant molecules. Dodecylammonuim bromide (DABr), dodecylmethylammonium bromide (DMABr), dodecyldimethylammonium bromide (DDMABr) were obtained from the reaction of dodecylamine, *N*-methyldodecylamine and *N*,*N*-dimethyldodecylamine, respectively, with $HBr_{(aq)}$. Diethylmethylamine and triethylamine were reacted with 1-bromododecane for the preparation of dodecyldiethylmethylammonium bromide (DDEMABr) and dodecyltriethylammonium bromide (DTEABr) as follows. A two-fold molar excess of the alkylamine was mixed with 1-bromododecane in ethanol and refluxed. The progress of the reactions was monitored by thin-layer chromatography carried out on 0.25 mm silica gel plates (60F-254) using UV light as visualizing agent, and $KMnO_4$ solution and heat as developing agents. After the reaction was completed, a yellow two-phase mixture was obtained. This mixture was concentrated by rotary evaporation. After precipitation by ether and subsequent filtration a solid residue was obtained. Sometimes the mixture had to be chilled to obtain precipitation. This solid residue was then purified by recrystallization from chloroform-ether, and subsequent filtration followed by drying under vacuum resulted in surfactants as white solids. All dodecylalkylammonium bromide surfactants, DAABr, (synthesized and purchased ones, Fig. 1) were characterized by ^{1}H nuclear magnetic resonance (^{1}H NMR) and Fourier transform infrared (FTIR) spectroscopy techniques. ^{1}H NMR spectra were recorded on JEOL NMR spectrometer (400 MHz) at ambient temperature. All chemical shifts (δ) are reported in part per million (ppm) downfield from TMS. The abbreviations used for NMR signals are: s = singlet, t = triplet, q = quartet, m = multiplet, br s = broad singlet, br m = broad multiplet. Infrared spectra were recorded on a Shimadzu IR prestige-21 FTIR. The NMR results, including commercially available ones for the comparison, are given in the following.

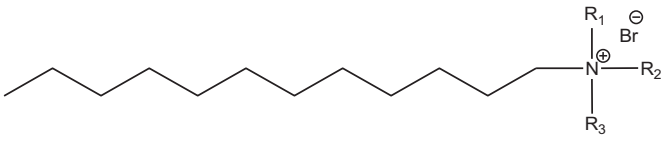

Fig. 1. Molecular structures of DAABr: $R_1 = R_2 = R_3 = -H$ for DABr; $R_1 = R_2 = -H$ and $R_3 = -CH_3$ for DMABr; $R_1 = -H$ and $R_2 = R_3 = -CH_3$ for DDMABr; $R_1 = R_2 = R_3 = -CH_3$ for DTMABr; $R_1 = R_2 = -CH_3$ and $R_3 = -CH_2CH_3$ for DDMEABr; $R_1 = -CH_3$ and $R_2 = R_3 = -CH_2CH_3$ for DDEMABr; $R_1 = R_2 = R_3 = -CH_2CH_3$ for DTEABr.

2.2.1. ^1H NMR (400 MHz)

Dodecylammonium bromide (DABr), δ (ppm, $CDCl_3$): 0.86 (CH_3, 3H, t), 1.23–1.30 (CH_2, 16H, br m), 1.34–1.41 (CH_2, 2H, m), 1.75–1.83 (CH_2, 2H, m), 3.02 (N^+CH_2, 2H, t), 7.92 (N^+H_3, 3H, br s).

Dodecylmethylammonium bromide (DMABr), δ (ppm, $CDCl_3$): 0.84 (CH_3, 3H, t), 1.21–1.28 (CH_2, 16H, br m), 1.31–1.41 (CH_2, 2H, m), 1.81–1.89 (CH_2, 2H, m), 2.65 (N^+CH_3, 3H, t), 2.93 (N^+CH_2, 2H, br t), 8.92 (N^+H_2, 2H, br s).

Dodecyldimethylammonium bromide (DDMABr), δ (ppm, $CDCl_3$): 0.83 (CH_3, 3H, t), 1.20–1.29 (CH_2, 18H, br m), 1.78–1.86 (CH_2, 2H, m), 2.79 (N^+CH_3, 6H, t), 2.99 (N^+CH_2, 2H, t), 11.17 (N^+H, 1H, br s).

Dodecyltrimethylammonium bromide (DTMABr), δ (ppm, $CDCl_3$): 0.83 (CH_3, 3H, t), 1.20 (CH_2, 14H, br m), 1.30 (CH_2, 4H, br m), 1.70 (CH_2, 2H, br m), 3.40 (N^+CH_3, 9H, s), 3.55 (N^+CH_2, 2H, t).

Dodecyldimethylethylammonium bromide (DDMEABr), δ (ppm, $CDCl_3$): 0.81 (CH_3, 3H, t), 1.18 (CH_2, 14H, br m), 1.29 (CH_2, 2H,br m), 1.34 (CH_3, 3H, t), 1.65 (CH_2, 2H, br m), 3.33 (N^+CH_3, 6H, s), 3.45 (N^+CH_2, 2H, t), 3.66 (N^+CH_2, 2H, q).

Dodecyldiethylmethylammonium bromide (DDEMABr), δ (ppm, $CDCl_3$): 0.82 (CH_3, 3H, t), 1.19–1.30 (CH_2, 18H, br m), 1.34 (CH_3, 6H, t), 1.60–1.67 (CH_2, 2H, m), 3.22 (CH_3, 3H, s), 3.34 (N^+CH_2, 2H, t), 3.57 (N^+CH_2, 4H, q).

Dodecyltriethylammonium bromide (DTEABr), δ (ppm, $CDCl_3$): 0.82 (CH_3, 3H, t), 1.19 (CH_2, 18H, br m), 1.33 (CH_3, 9H, t), 1.59–1.67 (CH_2, 2H, m), 3.21 (N^+CH_2, 2H, t), 3.46 (N^+CH_2, 6H, q).

2.3. Preparation of lyotropic liquid crystal samples

Lyotropic liquid crystalline mixtures were prepared into well-closed glass test tubes and then well-homogenized by applying vortex and centrifuging at 25 °C with a temperature-controlled centrifuge. A small amount of water-based ferrofluid (Ferrotec) was added into the samples, at a concentration of 1 μL per 1 g of the mixture, to obtain well-oriented nematic samples in the presence of an external magnetic field for the measurements of polarizing optical microscopy, laser conoscopy and small-angle X-ray scattering.

2.4. Experimental techniques

Polarizing optical microscopy was used to observe the textures and measure the transition temperatures of the different lyotropic liquid crystalline phases, using a microscope Eclipse E200POL (Nikon, Japan). The usual procedure is described elsewhere [11].

Laser conoscopy was employed to measure the two optical birefringences Δn and δn as functions of temperature in the three nematic phases of well-oriented samples in an external magnetic field. The optical birefringences are written as by $\Delta n = n_2 - n_1$ and $\delta n = n_3 - n_2$, where n_1, n_2 and n_3 are the principal refractive indices of the medium along the 1, 2 and 3 axes of the laboratory frame. This technique was used to unambiguously identify each nematic phase, to determine the nematic uniaxial to biaxial phase transition temperatures and the order of these transitions. The experimental setup and procedures, as well as the samples' alignment procedure in the magnetic field, were previously described [11,59,60].

Small-angle X-ray scattering (SAXS) was employed to measure and calculate, in the framework of a model-based analysis, the structural parameters of the samples in their respective nematic phases. The experimental setup, measurements' procedures, data treatment, and model used for data analysis were detailed described in the Supporting Information of [55].

3. Results and discussions

It is known that the interactions between ionic species on the micelles' surfaces affect the stabilization of different lyotropic nematic phases by modifying the packing of the surfactant molecules in the micelles, the surface curvature of the micelles, and the micellar shape anisotropy [11,33]. By modifying those interactions, the stabilization of different nematic phases becomes possible. Moreover, the temperature range of the N_B phase in the partial phase diagrams can be controlled. This can be done mainly in two ways, by considering the kosmotropic and the chaotropic (preference to be more or less hydrated by water molecules, respectively) properties of the surfactant head groups and of the counterions or ions of the electrolytes present in the lyotropic mixtures: (a) using a surfactant and choosing ions with different degree of the kosmotropic or chaotropic character with respect to it [22,24]; or (b) using surfactants with different head-group sizes to change the degree of the kosmotropic or chaotropic character of the surfactant head group and known electrolyte ion [11]. The latter way was followed in the present study. Thus, the interactions between the SSY, which has chaotropic character with two ionic groups at its periphery, and dodecylalkylammonium bromide surfactants with different head group character will be investigated.

The host mixture DTMABr/SSY/1-dodecanol/water (s4) was chosen [55] and its composition is given in Table 1. As it is known, the head group of DTMABr, $-N(CH_3)_3^+$, has a chaotropic character [61]. From DTMABr to DABr, the head groups turn into less chaotropic, while the head groups turn into more chaotropic from DTMABr to DTEABr. When DTMABr was completely replaced by other surfactants (e.g., DTEABr/SSY/1-dodecanol/water), their mixtures could not stabilize three nematic phases. Considering the concentrations of substances in sample s4, with DABr or DMABr, we did not get any homogeneous mixture. With DDMABr, a lamellar phase (L) was obtained (Fig. 2a). DDMEABr stabilized only the N_C phase (Fig. 2b), while a hexagonal phase (H) was observed in the mixtures of DDEMABr and DTEABr (Fig. 2c and d). Because a complete replacement of DTMABr with other surfactants did not stabilize the three nematic phases, mixtures with two main surfactants were prepared by replacing 2.5% portions of DTMABr, in mole fraction, with other dodecylalkylammonium bromides (DAABr), at total constant surfactant concentrations. In this way, we allowed the micelle surfaces to be covered by larger or smaller number of the chaotropic surfactant heads. The frontiers of the nematic phases' regions in the partial phase diagrams for DTMABr/DAABr binary mixtures were determined from their texture analysis by polarizing optical microscopy. The lyotropic nematic phases exhibited the characteristic "schlieren" textures. At lower temperatures, approximately below 13 °C, a gel-like phase was observed in all samples [55]. At higher temperatures, first a nematic to nematic-isotropic phase coexistence (2P) transition was observed, and then, by further increasing the temperature, a 2P to isotropic phase (I) transition was observed. The 2P regions were rich in isotropic phase. The nematic to nematic phase transition temperatures were determined by laser conoscopy and the temperature ranges of the N_B phase are given in Table 1.

Table 1 and Fig. 3 clearly show that, as the number of the $-CH_2$ groups in the surfactant head groups from samples s1 to s7 increases, the N_D-N_B and N_B-N_C phase transition temperatures shift to the higher values. Furthermore, the N_C phase stabilization is favored while the N_D and N_B phase domains get narrow, within the working-temperature range. Some models were proposed in the literature to explain the stabilization mechanism of the lyotropic nematic phases [15,62,63], but one of them seems to be more appropriate to explain how the different nematic phases are stabilized. This model, so-called 'Intrinsically Biaxial Micelles', or IBM, model

Table 1
Mixtures' identifications, second main surfactant identifications, compositions in percent molar fraction (X), nematic to nematic phase transition temperatures, temperature range of the N_B phase in °C (ΔT_{NB}), and the average number of –CH_2 groups in the head groups – see Eq. 1 - (n_{avg}).

Mixture	DAABr	X_{DTMABr}	X_{DAABr}	X_{SSY}	X_{DDeOH}	X_{water}	Phase transitions	ΔT_{N_B}	n_{avg}
s1	DABr	4.856	0.125	0.132	1.792	93.095	$N_D \xrightarrow{14.95^\circ C} N_B$	–	2.93
s2	DMABr	4.856	0.125	0.132	1.792	93.095	$N_D \xrightarrow{15.70^\circ C} N_B$	–	2.95
s3	DDMABr	4.856	0.125	0.132	1.792	93.095	$N_D \xrightarrow{17.35^\circ C} N_B$	–	2.98
s4	–	4.981	0.000	0.132	1.792	93.095	$N_D \xrightarrow{21.15^\circ C} N_B \xrightarrow{17.05^\circ C} N_C$	4.10	3.00
s5	DDMEABr	4.856	0.125	0.132	1.792	93.095	$N_D \xrightarrow{21.35^\circ C} N_B \xrightarrow{17.65^\circ C} N_C$	3.70	3.03
s6	DDEMABr	4.856	0.125	0.132	1.792	93.095	$N_D \xrightarrow{21.85^\circ C} N_B \xrightarrow{18.65^\circ C} N_C$	3.20	3.05
s7	DTEABr	4.856	0.125	0.132	1.792	93.095	$N_D \xrightarrow{23.05^\circ C} N_B \xrightarrow{20.30^\circ C} N_C$	2.75	3.08

[62,63] assumes the micelles have orthorhombic symmetry in the three nematic phases and different orientational fluctuations are responsible for stabilizing the different nematic phases. In the IBM model, the micelles are sketched, in a first order approximation, as rectangular parallelepipeds (or a flatted prolate ellipsoid), with average dimensions A′, B′ and C′, where C′ represents the micelle bilayer thickness. The orientational fluctuations around the axis perpendicular to the A′ × B′ plane lead to the stabilization of the N_D phase, and those around the axis parallel to the dimension A′ favor the stabilization of the N_C phase. The N_B phase is stabilized when only small-amplitude orientational fluctuations exist around the three orthogonal symmetry axes of the micelles. Considering the IBM model and the results of samples s1 to s7, by increasing the head-group size of the dodecylalkylammonium bromide surfactants, the orientational fluctuations responsible for the stabilization of the N_C phase overcome the orientational fluctuations for the stabilization of the N_D phase. Furthermore, the temperature range of the N_B phase (ΔT_{NB}) gets smaller, as shown in Fig. 4. In Fig. 4, ΔT_{NB} was plotted as a function of the average number of –CH_2 groups in the head groups (n_{avg}), calculated from Eq. 1:

$$n_{avg} = \frac{X_{DTMABr}}{X_{total}} n_{DTMABr} + \frac{X_{DAABr}}{X_{total}} n_{DAABr} \quad (1)$$

where n_{DTMABr} and n_{DAABr} are the numbers of the –CH_2 groups in the head groups of DTMABr and other dodecylalkylammonium bromides, respectively. n_{avg} for all samples are shown in Tables 1 and 3.

The micelle surface curvature is expected to increase in the sequence from lamellar to N_D, N_B, N_C, hexagonal and isotropic phases [64–66]. This may be attributed to the increase in the repulsions between the head groups and/or increase in the head-group size of the surfactant. Two factors are important to obtain different lyotropic structures, the temperature and the relative concentrations of the constituents of the mixture. In our case, constituents' concentrations were kept constant. When temperature increases, the phase sequence is N_C, N_B and N_D for the mixtures s4 to s7. It means that, as the temperature increases, the micelle surface curvature gets flatter due to charge screening between the ionic head groups of the surfactants on the micelle surfaces. This screening can only be provided by binding larger number of ionic species, counterions of the surfactants and/or ions of electrolytes present in the mixture. However, it was reported for the isotropic micellar solutions of DTMABr/water that the degree of counterion binding to the micelle decreases with the increase in the temperature [67,68]. Because the structural units of lyotropic systems are micelles, similar to the isotropic micellar solutions, experimental studies indicated that the information obtained from latter one can be applied to the former [23,24,33–37,69]. Our results can be interpreted as follows. When the temperature increases, a fewer number of counterions, Br^-, is bound to the micelle surface. Assuming that, at least, some number of SSY anionic part is bound instead of Br^-, the dye-surfactant interactions get stronger to stabilize the N_D phase. This happens by screening of repulsions between the head groups of the dodecylalkylammonium bromides rather than Br^-

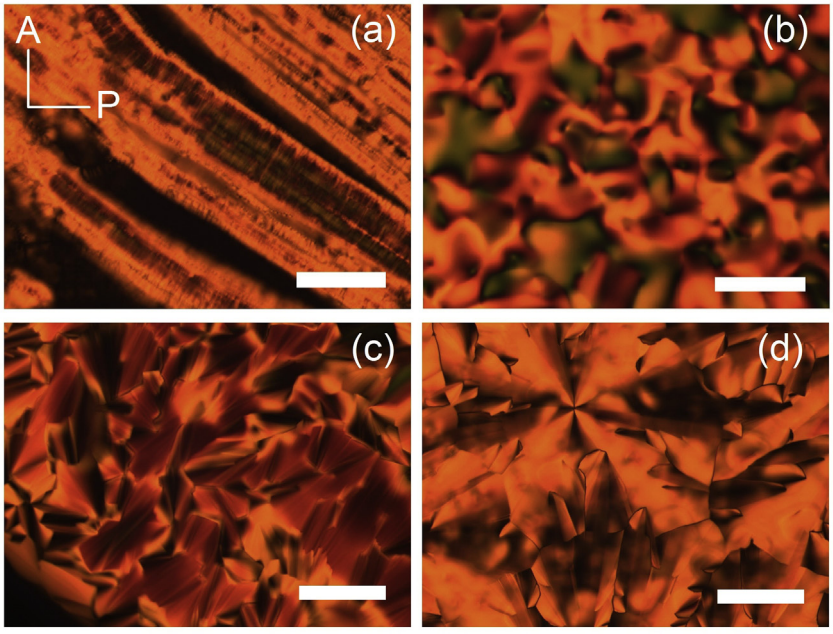

Fig. 2. Textures of (a) lamellar phase of DDMABr; (b) N_C phase of DDMEABr; and 2D-hexagonal phases of (c) DDEMABr and (d) DTEABr. A and P show the directions of the analyzer and the polarizer, respectively. The long axis of the flat capillary was at 45° to both A and P. The white bar corresponds to 200 μm. The sample thicknesses are 200 μm.

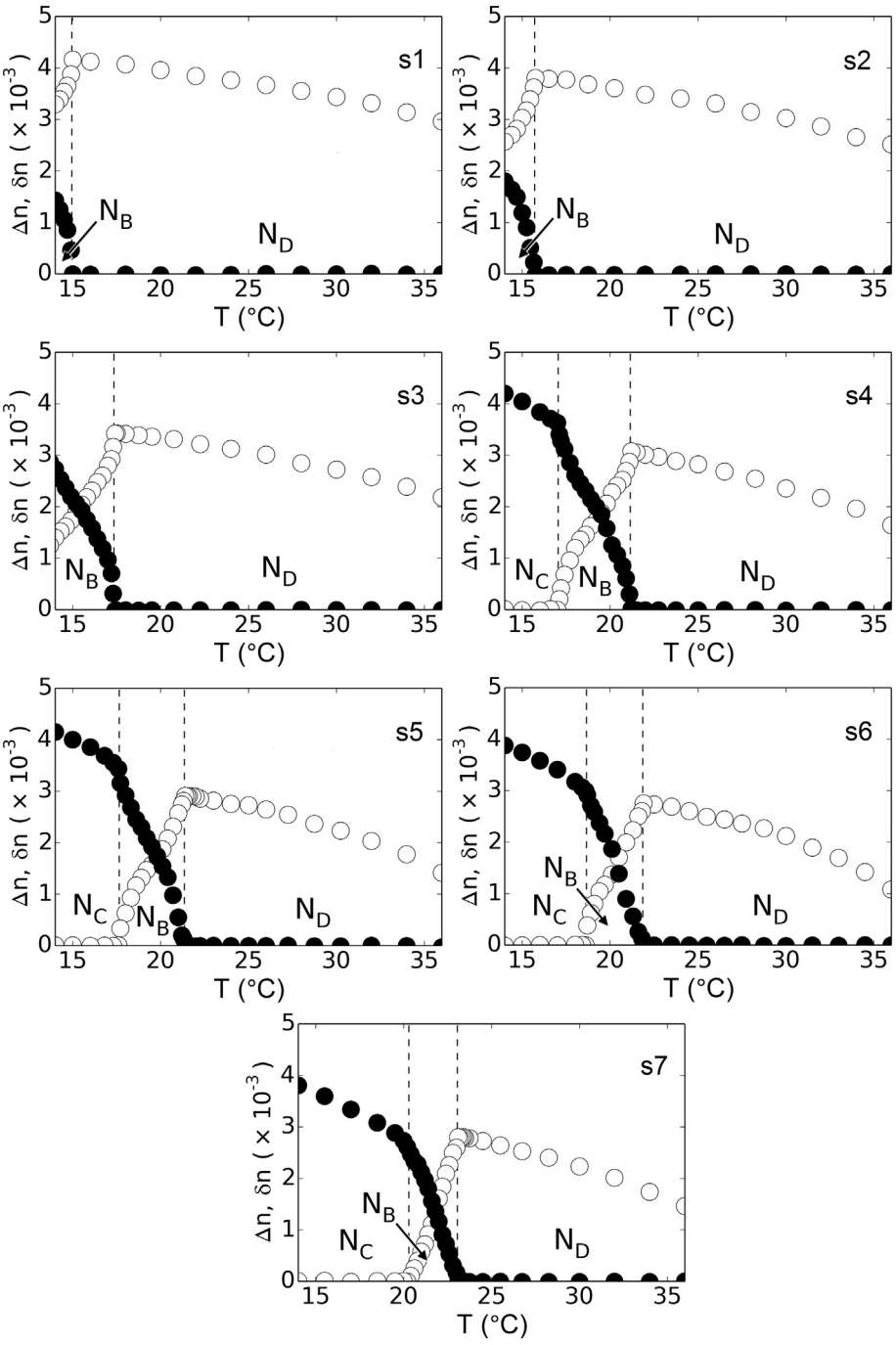

Fig. 3. Birefringences $\Delta n = n_2 - n_1$ (●) and $\delta n = n_3 - n_2$ (○) as functions of the temperature for mixtures given in Table 1.

counterions. This is an expected result because in our very recent study it was shown that SSY has bigger chaotropic character than Br^-, and the interactions between SSY and $DTMA^+$ head groups are stronger than those between Br^- and $DTMA^+$ [55]. Thus, the laser conoscopy results shown in Fig. 3 show that the dye-surfactant interactions control the stabilization of different nematic phases better than the conventional inorganic ions considering their chaotropic character. Furthermore, according to the IBM model, as the temperature increases, the SSY-binding to the micelle surface causes the micelle growth in the $A' \times B'$ plane, which favors the orientational fluctuations around the axis perpendicular to that plane, and the N_D phase was observed.

In the case of constant temperature and relative concentration of the substances, for instance, at about 14 °C, the micelle surfaces are more chaotropic going from s1 to s7, i.e. from DABr to DTEABr. Indeed, chaotropic or kosmotropic character is directly related to the ratio of charge/diameter or charge per surface area of the ionic species [44]. As expected, the apparent charge on the micelles [70] decreases from DABr to DTEABr. For instance, it was reported that the values of the apparent charges on the micelles are 15 ± 1 and 6 ± 1 for DTMABr and DTEABr under same conditions, respectively [71]. At 14 °C, the samples s1 to s3 stabilized the N_D and N_B phases but not the N_C. From s4 to s7, the samples exhibited the N_C phase in addition to the N_D and N_B. At constant temperature and relative concentrations, while the surfactant headgroup size of dodecylalkylammonium bromides gets larger (smaller), the N_C (N_D/N_B) phase stabilization is favored due to weakening (strengthening) of the dye-surfactant interaction between the head

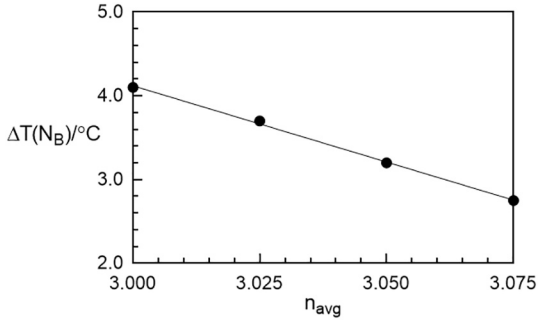

Fig. 4. Temperature range of the N_B phase (ΔT_{N_B}) as a function of the average number of –CH_2 groups in the head groups (n_{avg}) for the binary main surfactant mixtures of dodecylalkylammonium bromides. Solid line represents a linear fit.

groups and the anionic parts of SSY molecules on the micelle surfaces. This also shows that the chaotropic character of the SSY molecule is similar to that of DDMABr rather than DTMABr because, as the surfactants and ions have similar character, the N_D and/or N_B phases stabilization are highly possible [24]. Considering the IBM model, the SSY/DAABr interactions play a crucial role depending on the surfactant head-group sizes to control the orientational fluctuations responsible to obtain different nematic phases. The interactions between the smaller surfactant head groups than DTMABr and SSY dominantly favor the micelle growth in the A′ × B′ plane. This situation is confirmed by SAXS data given in Table 2. The dimension in the A′ × B′ plane decreases in the sequence DABr>DMABr>DDMABr>DTMABr. However, in the case of the surfactants which have higher chaotropic character with respect to DTMABr, the dimension of the A′ × B′ plane is almost unchanged. This may be attributed to the relatively weakly SSY-binding to the micelle surfaces, which favors the orientational fluctuations along the axis parallel to the A′ direction, to give the larger N_C phase domain.

If we compare the host mixture, s4, with others from Table 1, the addition or removal of the same number of –CH_2 group in the head group of DTMABr affects the nematic phase properties differently, e.g., nematic-nematic phase transitions and the nematic-phase domains in the phase diagrams. For instance, when 2.5% of DTMABr was replaced by DDMABr at constant total mixture' concentration, i.e., removal of one –CH_2 group in the head group, the N_D-N_B phase transition temperature changed ~3.8 °C and the N_C phase was not observed anymore. However, when same amount of DTMABr was replaced by DDMEABr, i.e., addition of one –CH_2 group in the head group, the N_D-N_B and N_B-N_C transitions were shifted only 0.2 °C and 0.6 °C, respectively. Similar situation can be seen for other mixtures. To clarify the reason why the removal of –CH_2 group from the head group affects the nematic phase properties more than the addition of –CH_2 group to the head group, additional samples were studied by preparing binary-surfactant mixtures of DTMABr/DDMABr and DTMABr/DDMEABr, where the relative concentrations of these two substances were changed, keeping the total surfactant concentration constant (Table 3). Fig. 5 shows the birefringences as a function of the temperature for these mixtures. The partial phase diagram was constructed considering the average number of the –CH_2 group in the head groups, Fig. 6. Furthermore, the change in ΔT_{NB} is plotted in Fig. 7.

The partial phase diagram clearly shows that the extent of surfactant-dye interactions is one of the factors that affects the stabilization of different nematic phases. Remember that the strong (weak) interactions between ionic species with similar (opposite) characters, in terms of kosmotropic and chaotropic, favor the stabilization of lyotropic N_D (N_C) phase [24].

The structural parameters of the samples given in Table 3 were also evaluated from the SAXS measurements (Table 4). The results are similar to those observed for other samples (Table 2). At a constant temperature (Fig. 6), as the head-group size of dodecylalkylammonium bromide increases, the shape anisotropy of the micelles decreases (Table 4) and the N_C phase is stabilized.

To interpret the effect of the head-group size dependence of the dye-surfactant interactions on obtaining different lyotropic nematic phases, a complete comparison considering the SAXS results of all mixtures studied according to the n_{avg} values is necessary and will be made in the following. The structural parameters were plotted as a function of the n_{avg} values of dodecylalkylammonium bromides, Fig. 8. The methodology used to obtain these parameters was described in Ref. [55]. Within the experimental error, the change in the structural parameters fits, in a first approach, to a linear behavior. The volume of surfactant chain (v) values in the calculation of the average surfactant packing parameter, v/a_0l, are obtained from Tanford's equation[72], $v = 27.4 + 26.9\ n_c$ in Å^3, where n_c is the number of carbon atoms in the alkyl chain of a surfactant molecule and its value is taken as 11 for all dodecylalkylammonium bromides, because one –CH_2 group is present in the head groups. Furthermore, the length of the alkyl chain, l, corresponds to half the micelle's core average bilayer thickness C′. The average a_0 was calculated in the model-based analysis of the SAXS results (Tables 2 and 4).

It is interesting to note that, although samples s2 and s9 consisted of different binary surfactants, DTMABr/DMABr with $X_{DMABr}/X_{total} = 2.5\%$ and DTMABr/DDMABr with $X_{DDMABr}/X_{total} = 5.0\%$, respectively, they have similar nematic to nematic phase transition temperatures, N_D–N_B is 15.70 °C for s2 and 15.05 °C for s9, and similar values of the structural parameters (Fig. 8), within the experimental error ($n_{avg} = 2.95$ for both samples). The samples s6 and s10 ($X_{DDEMABr}/X_{total} = 2.5\%$ and $X_{DDMEABr}/X_{total} = 5.0\%$) exhibited the same behavior ($n_{avg} = 3.05$). Furthermore, samples s6 and s10 gave very similar ΔT_{NB}, 3.20 °C for s6 and 3.60 °C for s10.

Table 5 summarizes the structural parameters' variations from $n_{avg} = 2.90$ to $n_{avg} = 3.15$. As the head-group size of the dodecylalkylammonium bromide increases the micellar dimensions A′ and B′ decrease about 16% and 12%, respectively, accompanying with the decrease in the N_{agg} (23%) and the SA (37%). This result seems to be due to the weakening of the surfactant-dye interactions on the micelle surfaces. Furthermore, the water layer around micelles gets thinner due to the hydration of the surfactant by less amount of water molecules which arises from the existence of the larger amount of chaotropic head groups at the micelle surfaces. Interestingly, although the decrease

Table 2
Structural parameters from SAXS measurements' results for samples given in Table 1. Mixture identification, micelle's core average dimensions (A′, B′, C′), average polar layer thickness (w), average aggregation number (N_{agg}), average area per polar head (a_0), average surfactant molecular packing parameter (v/a_0l), and shape anisotropy, SA = {[(A ' + B')/2 – C']/[(A ' + B')/2]}.

Mixture	A′ (Å)	B′ (Å)	C′ (Å)	w (Å)	N_{agg}	a_0 (Å^2)	v/a_0l	SA
s1	53.9 ± 2.3	38.3 ± 1.6	28.1 ± 1.4	15.2 ± 1.4	181 ± 6	51.6 ± 3.1	0.446 ± 0.035	0.39 ± 0.04
s2	51.4 ± 2.7	35.8 ± 1.8	28.7 ± 1.6	14.9 ± 1.6	165 ± 6	52.6 ± 3.8	0.428 ± 0.039	0.34 ± 0.04
s3	50.5 ± 2.6	35.4 ± 1.6	29.0 ± 1.5	14.7 ± 1.5	161 ± 6	53.0 ± 3.5	0.420 ± 0.035	0.33 ± 0.04
s4	46.9 ± 1.5	35.2 ± 1.1	29.4 ± 0.9	14.4 ± 0.9	150 ± 3	54.0 ± 2.4	0.407 ± 0.022	0.28 ± 0.03
s5	48.1 ± 2.1	34.8 ± 1.6	29.3 ± 1.3	14.5 ± 1.3	152 ± 5	53.8 ± 3.3	0.410 ± 0.031	0.29 ± 0.04
s6	48.4 ± 2.2	34.7 ± 1.4	29.2 ± 1.3	14.6 ± 1.3	153 ± 5	53.7 ± 3.2	0.412 ± 0.031	0.30 ± 0.04
s7	48.5 ± 2.5	34.4 ± 1.6	29.1 ± 1.5	14.5 ± 1.4	151 ± 5	54.0 ± 3.6	0.412 ± 0.035	0.30 ± 0.04

Table 3
Binary surfactant mixtures' compositions of DTMABr/DDMABr and DTMABr/DDMEABr in percent molar fraction (X), nematic-to-nematic phase transition temperatures, temperature range of the N_B phase in °C (ΔT_{NB}), and the average number of $-CH_2$ groups in the head groups (n_{avg}).

Mixture	X_{DTMABr}	X_{DDMABr}	$X_{DDMEABr}$	X_{SSY}	X_{DDeOH}	X_{water}	Phase transitions	ΔT_{NB}	n_{avg}
s8	4.482	0.499	–	0.132	1.792	93.095	N_D	–	2.90
s9	4.731	0.250	–	0.132	1.792	93.095	$N_D \xrightarrow{15.05^\circ C} N_B$	–	2.95
s3	4.856	0.125	–	0.132	1.792	93.095	$N_D \xrightarrow{17.35^\circ C} N_B$	–	2.98
s4	4.981	–	–	0.132	1.792	93.095	$N_D \xrightarrow{21.15^\circ C} N_B \xrightarrow{17.05^\circ C} N_C$	4.10	3.00
s5	4.856	–	0.125	0.132	1.792	93.095	$N_D \xrightarrow{21.35^\circ C} N_B \xrightarrow{17.65^\circ C} N_C$	3.70	3.03
s10	4.731	–	0.250	0.132	1.792	93.095	$N_D \xrightarrow{22.15^\circ C} N_B \xrightarrow{18.55^\circ C} N_C$	3.60	3.05
s11	4.482	–	0.499	0.132	1.792	93.095	$N_D \xrightarrow{22.85^\circ C} N_B \xrightarrow{20.45^\circ C} N_C$	2.40	3.10
s12	4.233	–	0.748	0.132	1.792	93.095	$N_D \xrightarrow{24.20^\circ C} N_B \xrightarrow{22.75^\circ C} N_C$	1.45	3.15
s13	3.984	–	0.997	0.132	1.792	93.095	$N_D \xrightarrow{24.45^\circ C} N_B \xrightarrow{23.35^\circ C} N_C$	1.10	3.20
s14	3.734	–	1.247	0.132	1.792	93.095	$N_D \xrightarrow{25.95^\circ C} N_B \xrightarrow{25.50^\circ C} N_C$	0.45	3.25
s15	3.484	–	1.497	0.132	1.792	93.095	N_C	–	3.30

in the thickness of the water layer (Fig. 8d) is observed, the micelle bilayer thickness (Fig. 8c) increases. It may be attributed to the increase in the average area per surfactant head group, a_0 (Fig. 8f). Mitchel and co-workers [65] discussed the relationship between the micelle shape, or lyotropic structure, and a_0: if $a_0 < 47$ Å^2 the lamellar structure is stabilized; if 70 Å^2 > a_0 ≥ 47 Å^2, the nematic phase (rod or disc-like

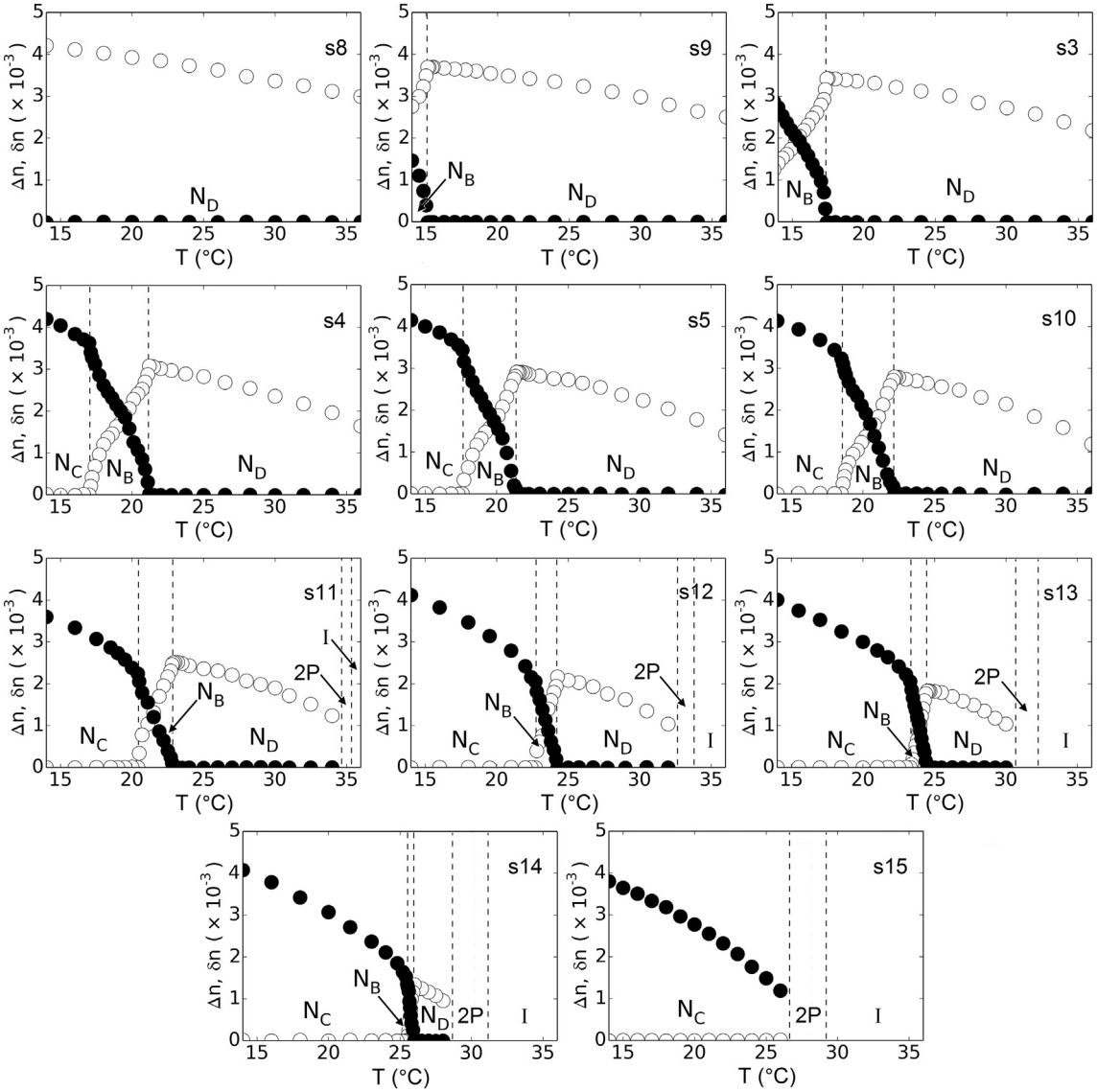

Fig. 5. Birefringences $\Delta n = n_2 - n_1$ (●) and $\delta n = n_3 - n_2$ (○) as a function of the temperature for mixtures given in Table 3.

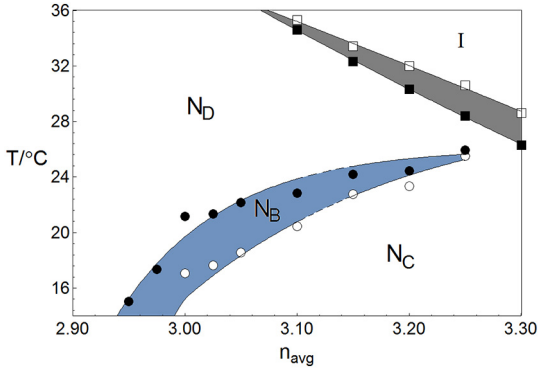

Fig. 6. Partial phase diagram of mixtures of Table 3 as a function of the average number of –CH_2 groups in the head groups of dodecylalkylammonium bromides. Grey region corresponds to two-phase region, i.e., coexistence of nematic and isotropic phase.

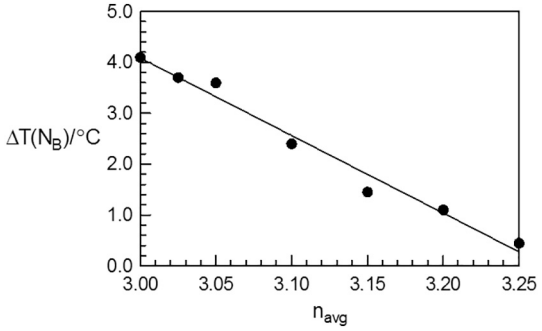

Fig. 7. Dependence of the temperature range of the N_B phase (ΔT_{N_B}) in the partial phase diagram on the average number of –CH_2 groups in the head groups of dodecylalkylammonium bromides. Solid line represents a linear fit.

micelles) is stabilized; if $a_0 > 70$ Å^2 isotropic micellar or hexagonal phases are stabilized (spheres, rod or discs). The a_0 values obtained in Mitchel's et al. study is exactly in the range from 47 to 70 Å^2, near the one for the nematic phases. In addition, for the N_D phase, it was reported that the a_0 is about 44–47 Å^2 [66]. According to Tables 2 and 4, 52 Å$^2 \geq a_0 >$ 57 Å^2 for a lyotropic mixture to show the biaxial nematic phase. Combining our results with those from [65,66], it is most likely to obtain only N_D and only N_C phases, if 52 Å$^2 > a_0 \geq$ 47 Å^2 and 70 Å$^2 > a_0 \geq$ 57 Å^2, respectively.

The IBM model, as we described in the previous sections, assumes two important parameters to explain the stabilization mechanism of different nematic phases: micelle symmetry or shape anisotropy, and orientational fluctuations. In previous studies [11,24] we qualitatively proposed that the micelle surface curvature should be different in each nematic phase. Here, the SAXS results quantitatively show that the micelle surface curvature is also an important parameter for obtaining the different nematic phases. Dawin et al. [33] experimentally showed that the packing parameter from lamellar to nematic phase and from nematic to isotropic phase decreases. Moreover, it is known that the micelle curvature increases in the sequence of lamellar → nematic → isotropic. They calculated the packing parameter, i.e., v/a_0l, at the nematic to lamellar transition as 0.55. Thus, it is clearly seen that the packing parameter is inversely proportional to the micelle surface curvature, i.e. the higher the packing parameter the smaller the micelle surface curvature. Table 5 indicates that, from the dodecylalkylammonium bromide with the lowest n_{avg} to the one with the highest n_{avg}, the packing parameter assumes smaller values. Possible extent of curvature and the value of the packing parameter to obtain the biaxial nematic phase, as well as some other lyotropic structures, are summarized in Fig. 9. It is well-known that if the packing parameter is lower than 1/3, the micelle surface has the highest micelle surface curvature and head-group area, and the aggregation of the surfactants molecules in the micelles is like a cone, Fig. 9a, i.e., the cross-section of the infinitively long micelles of the hexagonal phase. As the surfactant head-group size decreases the surfactant-aggregation type is a truncated cone, with smaller head-group size and medium extent of curvature, Fig. 9b, e.g., nematic phases. Finally, the surfactant aggregates in the lamellar phase show lowest surfactant head group and extent of curvature, Fig. 9c. Considering the classification of the a_0 values to obtain the uniaxial and biaxial nematic phases, we may generalize the packing parameter and extent of the curvature according to the laser conoscopy and especially SAXS results: only N_D phase was obtained from the s8 and it has the value of the packing parameter slightly smaller than ½, of 0.440; The value of the packing parameter for the sample s15, which gives only N_C phase, is 0.362 and this value is slightly higher than 1/3. So, we can make an assumption for obtaining the lyotropic biaxial nematic phase that $0.37 > v/a_0l > 0.44$. Consequently, it is seen that the packing parameter of the surfactant molecules in the micelles of the nematic phases is an important parameter to obtain different nematic phases. Thus, we may introduce to the IBM model that three nematic phases are composed of same kind of orthorhombic micelles with different micelle surface curvatures.

At this point we need to say somethings about an eventual relation between optical anisotropies and micelle surface curvature. In the biaxial phase temperature range, we experimentally observed that there is a temperature where $\Delta n = \delta n$. In terms of the invariants of the order parameter (the tensor optical dielectric tensor ε), their invariants (σ_i) are written as:

$$\varepsilon_{a1} = -\frac{4\langle n\rangle}{3}\left[\Delta n + \frac{\delta n}{2}\right]$$
$$\varepsilon_{a2} = \frac{2\langle n\rangle}{3}[\Delta n - \delta n]$$
$$\varepsilon_{a3} = \frac{4\langle n\rangle}{3}\left[\frac{\Delta n}{2} - \delta n\right]$$

$$\sigma_1 = 0$$
$$\sigma_2 = \frac{2}{3}\left({\varepsilon_{a1}}^2 + {\varepsilon_{a2}}^2 + {\varepsilon_{a3}}^2\right)$$
$$\sigma_3 = 4(\varepsilon_{a1}\varepsilon_{a2}\varepsilon_{a3})$$

Table 4
Structural parameters from SAXS measurements results for some samples listed in Table 3. Mixture identification, micelle's core average dimensions (A', B', C'), average polar layer thickness (w), average aggregation number (N_{agg}), average area per polar head (a_0), average surfactant molecular packing parameter (v/a_0l), and shape anisotropy (SA).

Mixture	A′ (Å)	B′ (Å)	C′ (Å)	w (Å)	N_{agg}	a_0 (Å^2)	v/a_0l	SA
s8	51.3 ± 1.6	39.2 ± 1.2	28.5 ± 1.0	15.1 ± 1.0	178 ± 4	51.6 ± 2.3	0.440 ± 0.025	0.37 ± 0.03
s9	51.4 ± 2.6	37.7 ± 1.9	28.5 ± 1.6	15.1 ± 1.6	173 ± 6	52.0 ± 3.7	0.437 ± 0.039	0.36 ± 0.04
s3	50.5 ± 2.6	35.4 ± 1.6	29.0 ± 1.5	14.7 ± 1.5	161 ± 6	53.0 ± 3.5	0.420 ± 0.035	0.33 ± 0.04
s4	46.9 ± 1.5	5.2 ± 1.1	29.4 ± 0.9	14.4 ± 0.9	150 ± 3	54.0 ± 2.4	0.407 ± 0.022	0.28 ± 0.03
s5	48.1 ± 2.1	34.8 ± 1.6	29.3 ± 1.3	14.5 ± 1.3	152 ± 5	53.8 ± 3.3	0.410 ± 0.031	0.29 ± 0.04
s10	46.4 ± 1.8	35.4 ± 1.1	29.3 ± 1.1	14.5 ± 1.1	150 ± 4	54.0 ± 2.7	0.409 ± 0.026	0.28 ± 0.03
s12	43.5 ± 1.4	34.4 ± 1.0	29.8 ± 0.9	14.2 ± 0.9	139 ± 3	55.1 ± 2.3	0.394 ± 0.020	0.23 ± 0.03

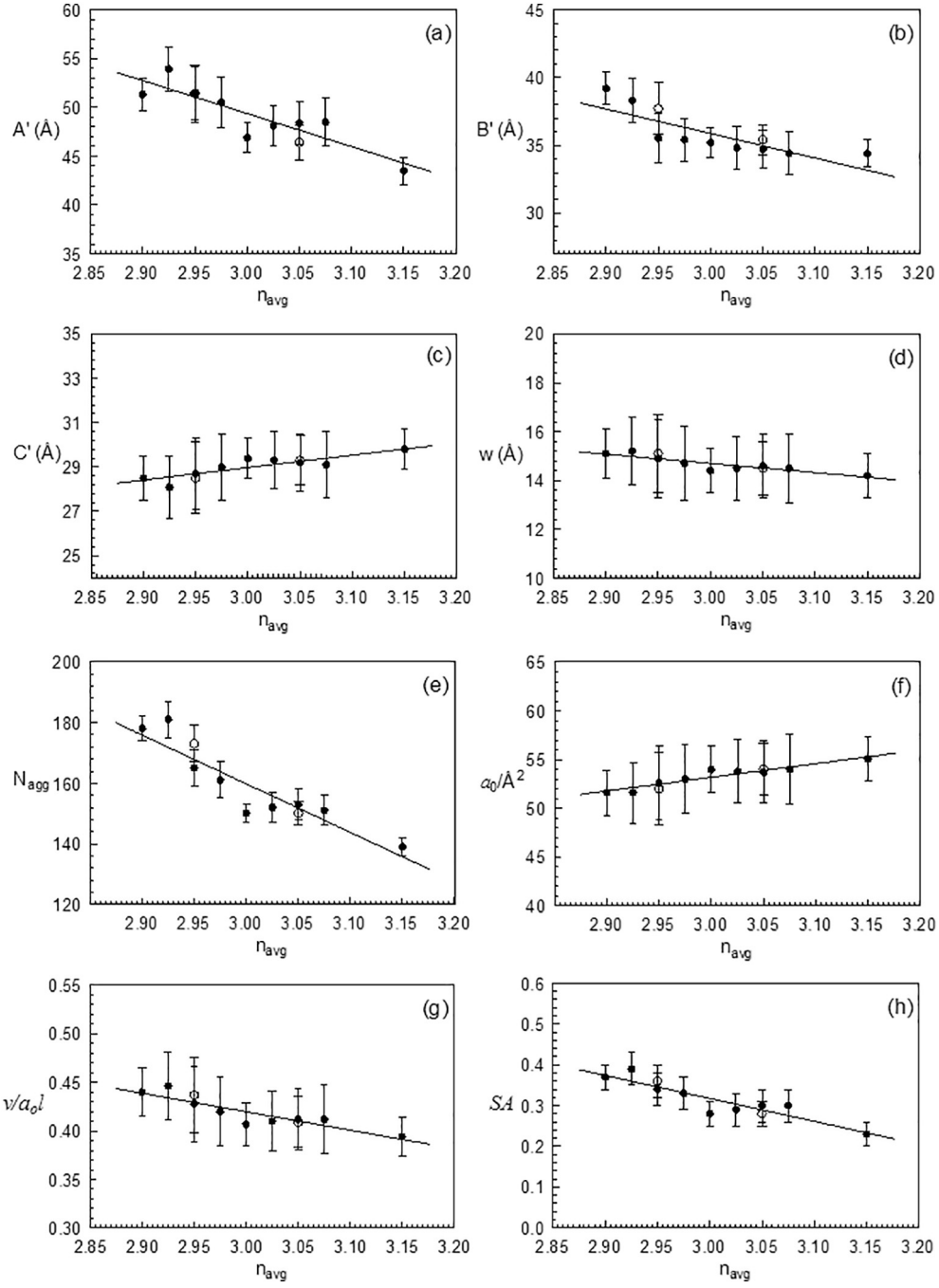

Fig. 8. Structural parameters of all samples as a function of n_{avg} of dodecylalkylammonium bromides. Samples s2 and s9, and s6 and s10 have the same n_{avg} values of 2.95 and 3.05, respectively, so that the parameters of s9 and s10 are represented by open-circles. Solid lines represent linear fits.

The laboratory frame axes are 1, 2 and 3. The orthorhombic micelle (e.g., a flattened ellipsoid) is oriented in this reference frame with the major radius parallel to the 1 axis, the smallest radius along the 3 axis and the medium axis along the 2 axis. In the N_D and N_C phase $\sigma_3 = {\sigma_2}^{3/2}$ and $\sigma_3 = -{\sigma_2}^{3/2}$, respectively. In the N_B phase $-{\sigma_2}^{3/2} < \sigma_3 < {\sigma_2}^{3/2}$. The temperature where $\Delta n = \delta n$ corresponds just to $\sigma_3 = 0$, i.e., $n_2 = \frac{n_1+n_3}{2}$, a mean value between n_1 and n_3. In other words, at this temperature, the optical anisotropies (Δn and δn) between the micellar medium along axis 2 and 1 equals that of the axis 3 and 2. There is no a simple relation between these optical anisotropies and the curvature in the micelle's surfaces and packing parameter, since the distribution of the main surfactant and co-surfactant is not homogeneous in the micelle (see, e.g., [73]). Our

Table 5
Change in the structural parameters, $(\chi_{final} - \chi_{initial})/\chi_{initial}$, where $\chi_{initial}$ and χ_{final} are the parameters at $n_{avg} = 2.90$ and $n_{avg} = 3.15$, respectively, from SAXS measurements for some samples listed in Tables 1 and 3. The values are obtained from the linear fit of the experimental values. The numbers in the parentheses are non-fitted experimental values.

χ	$n_{avg} = 2.90$	$n_{avg} = 3.15$	Change (%)
A′ (Å)	52.8 (51.3)	44.2 (43.5)	−16 (−19)
B′ (Å)	37.6 (39.2)	33.2 (34.4)	− 12 (−12)
C′ (Å)	28.4 (28.5)	29.8 (29.8)	+ 5 (+ 5)
w (Å)	15.0 (15.1)	14.1 (14.2)	− 6 (−6)
N_{agg}	176 (178)	136 (139)	− 23 (−22)
a_0 (Å^2)	51.8 (51.6)	55.1 (55.1)	+ 6 (+ 7)
v/a_0l	0.438 (0.440)	0.391 (0.394)	− 11 (−10)
SA	0.372 (0.370)	0.233 (0.230)	− 37 (−38)

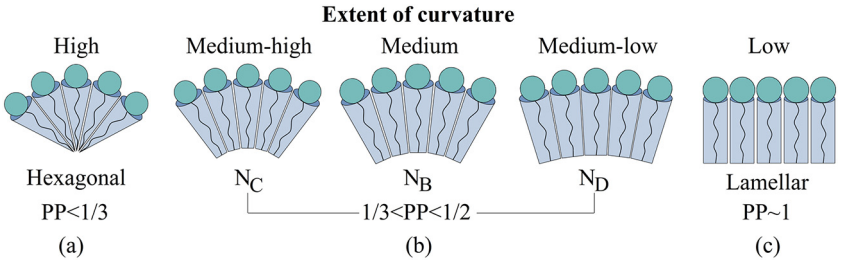

Fig. 9. Relationship between the micelle surface curvature and the packing parameter ($PP = v/a_0l$), and the expected lyotropic structures.

experimental evaluations of the micellar dimensions and packing parameter were (SAXS results) done at a fixed temperature (~25 °C). To be able to discuss the relation between the optical anisotropies and the micellar shape anisotropy and aggregation number (in particular when both birefringences equals), additional SAXS measurements will need to be performed, for a given sample, as a function of the temperature, and then compare with the conoscopy results, which will be a subject of another study.

4. Conclusions

We studied the effect of surfactant head-group size dependence of surfactant-dye interactions on the stabilization of different lyotropic nematic phases and nematic to nematic phase transitions. All experimental studies indicated that those interactions play a role in the stabilization of the uniaxial and biaxial nematic phases and phase transition temperatures by modifying the micellar structural parameters such as micelle' dimensions, average area per surfactant head group on the micelle surfaces, and micellar shape anisotropy. Furthermore, the surfactant packing parameter and the area per surfactant head group should have certain values for the stabilization of the nematic phases, especially the biaxial one. The IBM model, which explains the formation mechanism of the different nematic phases, needs to assume 'micelle surface curvature being different in three nematic phases' in addition to micelle symmetry and orientational fluctuations.

Author statement

The ***Authors*** certify that they have seen and approved the revised version of the manuscript being submitted.

Declaration of Competing Interest

None.

Acknowledgements

The authors thank the following scientific councils and agencies for supporting this work. From Turkey, the Scientific and Technological Research Council of Turkey (TÜBİTAK) [grant number: 217Z079] and Bolu Abant Izzet Baysal University Directorate of Research Projects Commission (BAP) [grant number 2020.03.03.1459]. From Brazil, the National Council for Scientific and Technological Development, the National Institute of Science and Technology Complex Fluids (INCT-FCx: 2014/50983-3), (NAP-FCx: 2011.1.9358.1.6) and the São Paulo Research Foundation (FAPESP-2018/07340-5 & 2016/24531-3) for supporting this work.

References

[1] Y. Hendrikx, J. Charvolin, Structural relations between lyotropic phases in the vicinity of the nematic phases, J. Phys. (France) 42 (1981) 1427–1440.
[2] B.J. Forrest, L.W. Reeves, New lyotropic liquid crystals composed of finite nonspherical micelles, Chem. Rev. 81 (1981) 1–14.
[3] F. Fujiwara, L.W. Reeves, M. Suzuki, J.A. Vanin, Solution Chemistry of Surfactants, Plenum Press, New York, 1979.
[4] L. Nasrin, E. Kabir, M. Rahman, External magnetic field-dependent tricritical points of uniaxial-to-biaxial nematic transition, Phase Transit. 89 (2016) 193–201.
[5] Y. Kim, B. Senyuk, S. Shin, A. Kohlmeier, G.H. Mehl, O.D. Lavrentovich, Surface alignment, anchoring transitions, optical properties, and topological defects in the thermotropic nematic phase of organo-siloxane tetrapodes, Soft Matter 10 (2014) 500–509.
[6] Y. Kim, G. Cukrov, F. Vita, E. Scharrer, E.T. Samulski, O. Francescangeli, O.D. Lavrentovich, Search for microscopic and macroscopic biaxiality in the cybotactic nematic phase of new oxadiazole bent-core mesogens, Phys. Rev. E 93 (2016), 062701, .
[7] A.M.F. Neto, S.R.A. Salinas, The Physics of Lyotropic Liquid Crystals: Phase Transitions and Structural Properties, Oxford University Press, New York, 2005.
[8] E. Akpinar, A.M.F. Neto, Experimental conditions for the stabilization of the lyotropic biaxial nematic mesophase, Crystals 9 (2019) 158.
[9] L.J. Yu, A. Saupe, Observation of a biaxial nematic phase in potassium laurate-1-decanol-water mixtures, Phys. Rev. Lett. 45 (1980) 1000–1003.
[10] R. Bartolino, T. Chiaranza, M. Meuti, R. Compagnoni, Uniaxial and biaxial lyotropic nematic liquid crystals, Phys. Rev. A 26 (1982) 1116–1119.
[11] E. Akpinar, E. Guner, O. Demir-Ordu, A.M.F. Neto, Effect of head-group size of some tetradecylalkylammonium bromide surfactants on obtaining the lyotropic biaxial nematic phase, Eur. Phys. J. E 42 (2019) 44.
[12] M.J. Freiser, Ordered states of a nematic liquid, Phys. Rev. Lett. 24 (1970) 1041–1043.
[13] R. Alben, Liquid crystal phase transitions in mixtures of rodlike and platelike molecules, J. Chem. Phys. 59 (1973) 4299–4304.
[14] E.A. Oliveira, L. Liebert, A.M.F. Neto, A new soap/detergent/water lyotropic liquid crystal with a biaxial nematic phase, Liq. Cryst. 5 (1989) 1669–1675.
[15] A. Stroobants, H.N.W. Lekkerkerker, Liquid crystal phase transitions in a solution of rodlike and disklike particles, J. Phys. Chem. 88 (1984) 3669–3674.
[16] Y. Galerne, J.P. Marcerou, Temperature behavior of the order-parameter invariants in the uniaxial and biaxial nematic phases of a lyotropic liquid crystal, Phys. Rev. Lett. 51 (1983) 2109–2111.
[17] C.C. Ho, R.J. Hoetz, M.S. El-Aasser, A biaxial lyotropic nematic phase in dilute solutions of sodium lauryl sulfate-1-hexadecanol-water, Langmuir 7 (1991) 630–635.
[18] P.P. Muhoray, J.R. Bruyn, D.A. Dunmur, Phase behavior of binary nematic liquid crystal mixtures, J. Chem. Phys. 82 (1985) 5294–5295.
[19] A.M. Filho, A. Laverde, F.Y. Fujiwara, Observation of two biaxial nematic mesophases in the tetradecyltrimethylammonium bromide/decanol/water system, Langmuir 19 (2003) 1127–1132.
[20] F.M. Kooij, H. Lekkerkerker, Liquid-crystal phases formed in mixed suspensions of rod- and platelike colloids, Langmuir 16 (2000) 10144–10149.
[21] E. Akpinar, D. Reis, A.M.F. Neto, Effect of alkyl chain length of alcohols on nematic uniaxial-to-biaxial phase transitions in a potassium laurate/alcohol/K_2SO_4/water lyotropic mixture, Liq. Cryst. 39 (7) (2012) 881–888.
[22] E. Akpinar, D. Reis, A.M.F. Neto, Effect of Hofmeister anions on the existence of the biaxial nematic phase in lyotropic mixtures of dodecyltrimethylammonium bromide/sodium salt/1-dodecanol/water, Liq. Cryst. 42 (7) (2015) 973–981.
[23] E. Akpinar, K. Otluoglu, M. Turkmen, C. Canioz, D. Reis, A.M.F. Neto, Effect of the presence of strong and weak electrolytes on the existence of uniaxial and biaxial nematic phases in lyotropic mixtures, Liq. Cryst. 43 (2016) 1693–1708.
[24] E. Akpinar, M. Turkmen, C. Canioz, A.M.F. Neto, Role of kosmotrope-chaotrope interactions at micelle surfaces on the stabilization of lyotropic nematic phases, Eur. Phys. J. E 39 (2016) 107.
[25] E. Akpinar, C. Canioz, M. Turkmen, D. Reis, A.M.F. Neto, Effect of the surfactant alkyl chain length on the stabilization of lyotropic nematic phases, Liq. Cryst. 45 (2) (2018) 219–229.
[26] D. Myers, Surfactant Science and Technology, John Wiley & Sons, New Jersey, 2006.
[27] B. Kumar, D. Tikariha, K.K. Ghosh, Effects of electrolytes on micellar and surface properties of some monomeric surfactants, J. Dispers. Sci. Technol. 33 (2012) 265–271.
[28] L. Rhein, Surfactant action on skin and hair: cleansing and skin reactivity mechanisms, Handbook for Cleaning/Decontamination of Surfaces, 1 2007, pp. 305–369.
[29] S.N. Miqan, F.F. Tabrizi, H. Abedini, H.A. Kashi, Estimation of micellization parameters of sds in the presence of some electrolytes for emulsion polymerization systems, J. Surfactant Deterg. 16 (2013) 271–278.

[30] K. Hac-Wydro, A. Mateja, A. Ożóg, P. Miśkowiec, Influence of metal ions on the aggregation of anionic surfactants. Studies on the interactions between environmental pollutants in aqueous solutions, J. Mol. Liq. 240 (2017) 514–521.
[31] C.M. Phan, M. Haseeb, Relative contribution of cationic surfactant and counter-anion to a liquid film tension, J. Mol. Liq. 306 (2020) 112802.
[32] Md R. Amin, S.A. Alissa, M. Saha, J. Hossian, I. Shahriar, M.A. Halim, Md A. Hoquea, Z.A. Alothman, S.M. Wabaidur, S.E. Kabir, Investigation of the impacts of temperature and electrolyte on the interaction of cationic surfactant with promethazine hydrochloride: Combined conductivity and molecular dynamics studies, J. Mol. Liq. 311 (2020) 113246.
[33] U.C. Dawin, J.P.F. Lagerwall, F. Giesselmann, Electrolyte effects on the stability of nematic and lamellar lyotropic liquid crystal phases: colligative and ion-specific aspects, J. Phys. Chem. B 113 (2009) 11414–11420.
[34] A. Sein, J.B.F.N. Engberts, Micelle to lamellar aggregate transition of an anionic surfactant in dilute aqueous solution induced by alkali metal chloride and tetraalkylammonium chloride salts, Langmuir 11 (1995) 455–465.
[35] C. Oelschlaeger, P. Suwita, N. Willenbacher, Effect of counterion binding efficiency on structure and dynamics of wormlike micelles, Langmuir 26 (2010) 7045–7053.
[36] V.K. Aswal, P.S. Goyal, Counterions in the growth of ionic micelles in aqueous electrolyte solutions: a small-angle neutron scattering study, Phys. Rev. E 61 (2000) 2947–2953.
[37] J.N. Israelachvili, Intermolecular and Surface Forces, 1st edition Academic Press, New York, 1991.
[38] M.S. Leaver, M.C. Holmes, A small angle neutron scattering study of the lamellar and nematic phases of caesium pentadecafluoro-octanoate (CsPFO)/^2H_2O and CsPFO/CsCl/ ^2H_2O, J. Phys. II 3 (1993) 105–120.
[39] M.C. Holmes, M.S. Leaver, A.M. Smith, Nematic and disrupted lamellar phases in cesium pentadecafluorooctanoate/^2H_2O: a small angle scattering study, Langmuir 11 (1995) 356–365.
[40] K.D. Collins, Ions from the Hofmeister series and osmolytes: effects on proteins in solution and in the crystallization process, Methods 34 (2004) 300–311.
[41] K.D. Collins, G.W. Neilson, J.E. Enderby, Ions in water: characterizing the forces that control chemical processes and biological structure, Biophys. Chem. 128 (2007) 95–104.
[42] B.E. Conway, Ionic Hydration in Chemistry and Biophysics, 1st edition Elsevier Scientific Publishing Company, The Netherlands, 1981.
[43] Y. Marcus, Ion Solvation, 1st edition John Wiley and Sons Ltd, London, 1985.
[44] K.D. Collins, Charge density-dependent strength of hydration and biological structure, Biophys. J. 72 (1997) 65–76.
[45] L. Moreira, A. Firoozabadi, Molecular thermodynamic modeling of specific ion effects on micellization of ionic surfactants, Langmuir 26 (2010) 15177–15191.
[46] S. Fazeli, B. Sohrabi, A.R. Tehrani-Bagha, The study of sunset yellow anionic dye interactionwith Gemini and conventional cationic surfactants in aqueous solution, Dyes Pigments 95 (2012) 768–775.
[47] R.T. Buwalda, J.B.F.N. Engberts, Aggregation of dicationic surfactants with methyl orange in aqueous solution, Langmuir 17 (2001) 1054–1059.
[48] S. Gokturk, M. Tuncay, Dye-surfactant interaction in the premicellar region, J. Surfactant Deterg. 6 (2003) 325–330.
[49] M.N. Khan, A. Sarwar, Study of dye–surfactant interaction: aggregation and dissolution of yellowish in N-dodecyl pyridinum chloride, Fluid Phase Equilib. 239 (2006) 166–171.
[50] A.A. Shahir, S. Javadian, M. Razavizadeh, H. Gharibi, Comprehensive study of tartrazine/cationic surfactant interaction, J. Phys. Chem. B 115 (2011) 14435–14444.
[51] S.T. Muntaha, M.N. Khan, Study of changes in conductivity and spectral behaviour before and after micelle formation in the dye-surfactant system, J. Mol. Liq. 197 (2014) 191–196.
[52] N. Erdinc, S. Gokturk, Spectrophotometric and conductometric studies on the interaction of anionic dye Eosin-Y with cationic micelles, Anal. Chem. Lett. 4 (2014) 146–157.
[53] M.T. Muhammad, M.N. Khan, Study of electrolytic effect on the interaction between anionic surfactant and methylene blue using spectrophotometric and conductivity methods, J. Mol. Liq. 234 (2017) 309–314.
[54] M.T. Muhammad, M.N. Khan, Oppositely charged dye surfactant interactions: extent and selectivity of ion pair formation, J. Mol. Liq. 266 (2018) 591–596.
[55] E. Akpinar, G. Topcu, D. Reis, A.M.F. Neto, Effect of the anionic azo dye sunset yellow in lyotropic mixtures with uniaxial and biaxial nematic phases, J. Mol. Liq. 318 (2020) 114010.
[56] X.-H. Cheng, Y. Peng, C. Gao, Y. Yan, J.-B. Huang, Studying of 1-D assemblies in anionic azo dyes and cationic surfactants, Colloids Surf. A: Physicochem. Eng. Aspects 422 (2013) 10–18.
[57] V.R. Horowitz, L.A. Janowitz, A.L. Modic, P.A. Heiney, P.J. Collings, Aggregation behavior and chromonic liquid crystal properties of an anionic monoazo dye, Phys. Rev. E 72 (2005), 041710, .
[58] H. Park, S. Kang, L. Tortora, Y. Nastishin, D. Finotello, S. Kumar, O.D. Lavrentovich, Self-assembly of lyotropic chromonic liquid crystal sunset yellow and effects of ionic additives, J. Phys. Chem. B 112 (2008) 16307–16319.
[59] E. Akpinar, D. Reis, A.M.F. Neto, Lyotropic mixture made of potassium laurate/1-undecanol/K2SO4/water presenting high birefringences and large biaxial nematic phase domain: a laser conoscopy study, Eur. Phys. J. E 35 (2012) 50.
[60] Y. Galerne, J.P. Marcerou, Temperature-concentration behaviour of the order parameter in the nematic phases of a lyotropic liquid crystal, J. Physique France 46 (1985) 589–594.
[61] Y. Marcus, Effect of ions on the structure of water: structure making and breaking, Chem. Rev. 109 (2009) 1346–1370.
[62] A.M.F. Neto, Y. Galerne, A.M. Levelut, L. Liebert, Pseudo-lamellar ordering in uniaxial and biaxial lyotropic nematics: a synchrotron X-ray diffraction experiment, J. Phys. Lett. (Paris) 46 (1985) 499–505.
[63] Y. Galerne, A.M.F. Neto, L. Liebert, Microscopical structure of the uniaxial and biaxial lyotropic nematics, J. Chem. Phys. 87 (1987) 1851–1856.
[64] E.S. Blackmore, G.J.T. Tiddy, Phase behaviour and lyotropic liquid crystals in cationic surfactant–water systems, J. Chem. Soc. Faraday Trans. 2 (84) (1988) 1115–1127.
[65] D.J. Mitchell, G.J.T. Tiddy, L. Waring, T. Bostock, M.P. McDonald, Phase behaviour of polyoxyethylene surfactants with water. Mesophase structures and partial miscibility (cloud points), J. Chem. Soc. Faraday Trans. 1 79 (1983) 975–1000.
[66] G.J.T. Tiddy, in: H.F. Eicke (Ed.), Modern Trends of Colloid Science in Chemistry and Biology, Birkhauser Verlag, Basel 1985, p. 148.
[67] S. Chauhan, K. Sharma, Effect of temperature and additives on the critical micelle concentration and thermodynamics of micelle formation of sodium dodecyl benzene sulfonate and dodecyltrimethylammonium bromide in aqueous solution: a conductometric study, J. Chem. Thermodyn. 71 (2014) 205–211.
[68] S. Chauhan, M. Kaur, K. Kumar, M.S. Chauhan, Study of the effect of electrolyte and temperature on the critical micelle concentration of dodecyltrimethylammonium bromide in aqueous medium, J. Chem. Thermodyn. 78 (2014) 175–181.
[69] E. Akpinar, S. Yurdakul, A.M.F. Neto, Comparison between lyotropic cholesteric phase behavior with partly fluorinated surfactants and their exact hydrogenated counterparts, J. Mol. Liq. 259 (2018) 239–248.
[70] S. Durand-Vidal, M. Jardat, V. Dahirel, O. Bernard, K. Perrigaud, P. Turq, Determining the radius and the apparent charge of a micelle from electrical conductivity measurements by using a transport theory: explicit equations for practical use, J. Phys. Chem. B 110 (2006) 15542–15547.
[71] R. Jaber, M.J. Wasbrough, J.A. Holdaway, K.J. Edler, Interactions between quaternary ammonium surfactants and polyethylenimine at high pH in film forming systems, J. Colloid Interface Sci. 449 (2015) 286–296.
[72] C. Tanford, The hydrophobic effect: Formation of Micelles and Biological Membranes, 2nd ed. Wiley, New York, 1980.
[73] Y. Hendrikx, J. Charvolin, M. Rawiso, Uniaxial-biaxial phase transition in lyotropic nematic solutions: local biaxiality in the uniaxial phase, Phys. Rev. B 33 (1986) 3534–3537.